

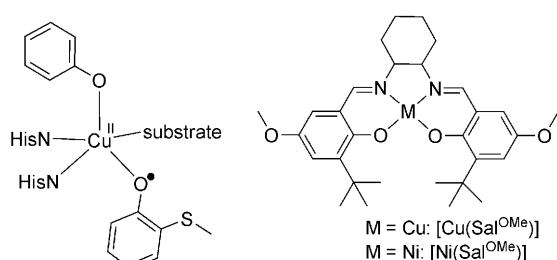
X-Ray Structures of Copper(II) and Nickel(II) Radical Salen Complexes: The Preference of Galactose Oxidase for Copper(II)

Maylis Orio, Olivier Jarjays, Hussein Kanso, Christian Philouze, Frank Neese, and Fabrice Thomas*

Organic radicals are normally extremely reactive, and often nonselective and toxic species. They are found in a number of proteins, some of which are involved in essential processes such as photosynthesis and DNA synthesis.^[1] Nature has therefore nicely succeeded in domesticating them and taking advantage of their high reactivity. Galactose oxidase (GO, Scheme 1), which catalyzes aerobic oxidation of primary

definitely confirm this assumption and reveal the structural changes associated with radical formation. We have now succeeded in obtaining the radical complex $[\text{Cu}(\text{Sal}^{\text{OMe}})]^+$ (Figure 1) as single crystals. Its structure is described below and compared to that of its nickel(II) analogue, which could be also crystallized.

Prior to preparing the radical species, the bis(phenolate) precursor $[\text{Cu}(\text{Sal}^{\text{OMe}})]$ was structurally characterized; the copper ion has an almost square-planar geometry. Its cyclic-



Scheme 1. Active site of galactose oxidase and model complexes.

alcohols to aldehydes, is one of these fascinating radical proteins. Its active site consists of a copper(II) ion coordinated to two histidine residues, one tyrosine residue, and a tyrosyl radical (Tyr_{272}^{\cdot}) essential for catalysis.^[2] Many complexes involving coordinated phenoxyl radicals were developed in the last ten years to gain insight into the copper-radical interaction. Unfortunately, most of them decompose so quickly that they must be generated in situ and characterized at low temperature.^[3] For these reasons, crystal structures of true phenoxyl radicals^[4] coordinated to transition metals are very rare.^[5–7]

Because they are functional mimics of the GO active site, one-electron oxidized Cu^{II} salen complexes (involving *o,p* sterically hindered phenolates) have received considerable interest.^[8–9] Spectroscopic investigations suggested the occurrence of a coordinated phenoxyl moiety in these complexes. However, no X-ray crystal structure is yet available to

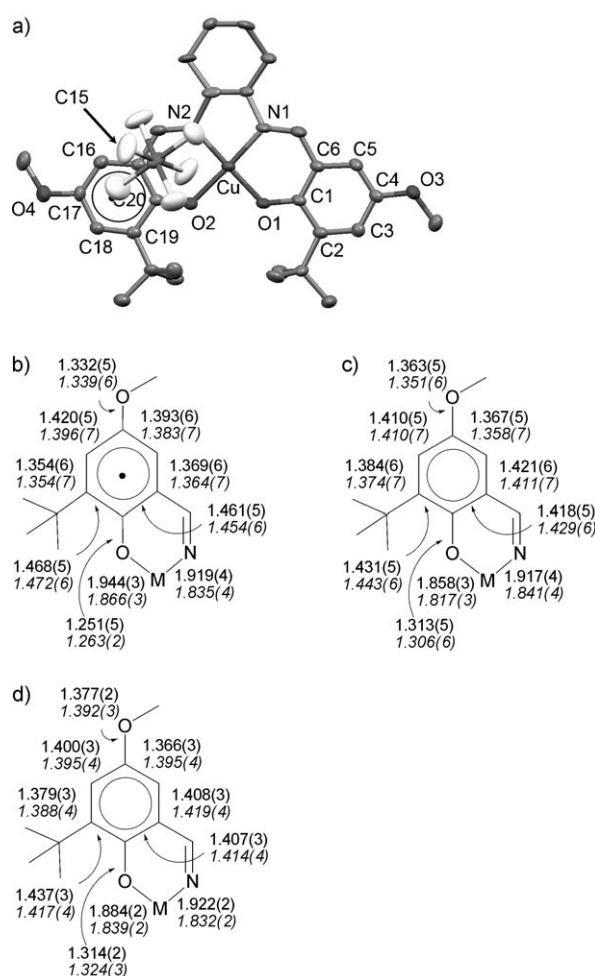


Figure 1. a) X-Ray crystal structure of $[\text{Cu}(\text{Sal}^{\text{OMe}})]^+\text{SbF}_6^-$ (thermal ellipsoids set at 50%). b, c) Selected bond lengths [Å] in the phenoxyl and phenolate rings, respectively, for $[\text{Cu}(\text{Sal}^{\text{OMe}})]^+\text{SbF}_6^-$ (standard text) and $[\text{Ni}(\text{Sal}^{\text{OMe}})]^+\text{SbF}_6^-$ (italics). d) Selected bond lengths [Å] in the neutral complexes $[\text{Cu}(\text{Sal}^{\text{OMe}})]$ (standard text) and $[\text{Ni}(\text{Sal}^{\text{OMe}})]$ (italics).

[*] Dr. O. Jarjays, H. Kanso, Dr. C. Philouze, Prof. F. Thomas
Département de Chimie Moléculaire, Chimie Inorganique, Redox
Biomimétique (CIRE), UMR CNRS 5250, Université Joseph Fourier
B.P. 53, 38041 Grenoble cedex 9 (France)
Fax: (+33) 4-7651-4836
E-mail: fabrice.thomas@ujf-grenoble.fr

Dr. M. Orio, Prof. F. Neese

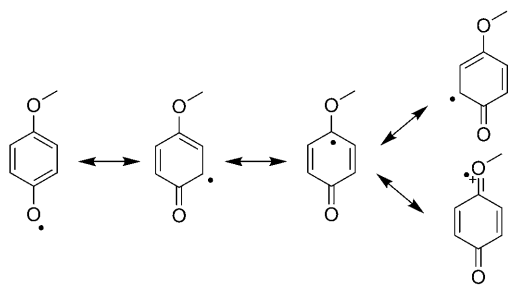
Institute for Physical and Theoretical Chemistry, Universität Bonn
Wegelerstrasse 12, 53113 Bonn (Germany)



Supporting information for this article is available on the WWW
under <http://dx.doi.org/10.1002/anie.201001040>.

voltammetry curve displays two reversible one-electron redox waves at $E_{1/2}^1 = +0.28$ and $E_{1/2}^2 = +0.44$ V versus ferrocene/ferrocenium (Fc/Fc^+) and is attributed to the formation of mono- and bis(phenoxy) radical species. Electrogenerated $[\text{Cu}(\text{Sal}^{\text{OMe}})]^+$ exhibits absorptions at 409 and 460 nm, as well as a broad band at $\lambda > 1100$ nm,^[10] which correspond to $\pi-\pi^*$ and charge-transfer transitions of phenoxy radicals.^[3] It is X-band EPR-silent, as expected for magnetic coupling between the radical and metal spins.

Single crystals of $[\text{Cu}(\text{Sal}^{\text{OMe}})]^+$ were obtained by oxidation of the neutral precursor with a silver salt^[11] and diffusion of pentane into the solution.^[7] A striking feature in the structure of $[\text{Cu}(\text{Sal}^{\text{OMe}})]^+$ is the nonequivalence in the Cu–O bond lengths (Figure 1): while the Cu–O1 bond length is 1.867(3) Å, that is, similar to the Cu–O bonds in $[\text{Cu}(\text{Sal}^{\text{OMe}})]$, the Cu–O2 bond is much longer (1.940(3) Å). Detailed investigation of the C–C and C–O bond lengths within the ring containing O1 reveals strong analogies with the phenolate moieties of $[\text{Cu}(\text{Sal}^{\text{OMe}})]$. In contrast, the bond lengths in the ring containing O2 exhibit new features. The C18–C19 and C15–C16 bonds are equivalent (1.342(7) and 1.350(7) Å, respectively) and dramatically shorter than the C15–C20, C16–C17, C17–C18, C19–C20 bonds (1.446(6), 1.393(6), 1.433(6) and 1.482(6) Å, respectively). In addition, the C19–O2 and C17–O4 bonds are about 0.05 Å shorter in $[\text{Cu}(\text{Sal}^{\text{OMe}})]^+$ with respect to the neutral precursor. These features are consistent with a quinoid structure for the ring containing the O2 atom, and thus a radical character for this moiety (Scheme 2).^[6] Finally, close contacts exist between the



Scheme 2. Canonical forms of *p*-methoxyphenoxyl radicals.

negatively charged counterion and the electron-deficient radical ring. This interaction likely contributes to localization of the radical on one ring and mimics the stabilizing interaction between Tyr_{272}^{\cdot} and Trp_{290} in the GO active site.^[2] Density functional calculations on $[\text{Cu}(\text{Sal}^{\text{OMe}})]^+\text{SbF}_6^-$ confirm the asymmetry of the complex: the spin densities at O2 (0.24) and N2 (0.20) are larger than those at O1 (0.20) and N1 (0.16). Similar analysis applies when comparing the spin populations within each aromatic ring. It is instructive to compare the structural features of $[\text{Cu}(\text{Sal}^{\text{OMe}})]^+\text{SbF}_6^-$ with those of $[\text{Cu}(\text{Sal}^{\text{Bu}})]^+\text{SbF}_6^-$, which has been identified as a copper(III) complex.^[12] The latter exhibits symmetrical Cu–O and Cu–N bonds which are much shorter (1.841 and 1.876 Å respectively). A weak interaction between $[\text{Cu}(\text{Sal}^{\text{Bu}})]^+$ and

the SbF_6^- counterion was detected, but in this case it occurs mainly through an axial Cu–F bond (2.76 Å) due to the symmetry of the molecule and the ligand demand of the Cu^{III} ion.

From these first structural data on a copper(II) radical salen complex, the nature of the magnetic interaction could be deduced. The metal-centered SOMO has $d_{x^2-y^2}$ character (square-planar copper), whereas the ligand SOMO is mainly developed on the aromatic ring close to SbF_6^- (65 % contribution). As shown in Figure 2 the $d_{x^2-y^2}$ and π -radical

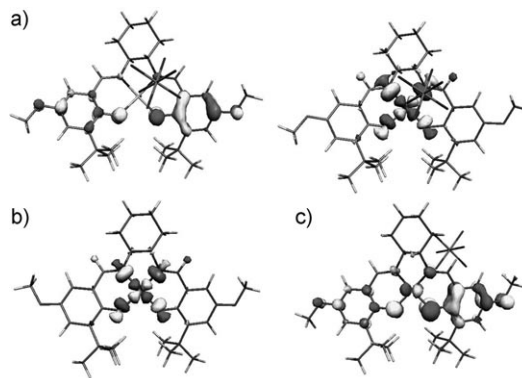


Figure 2. Localized SOMOs of a) $[\text{Cu}(\text{Sal}^{\text{OMe}})]^+\text{SbF}_6^-$, b) $[\text{Cu}(\text{Sal}^{\text{OMe}})]$, and c) $[\text{Ni}(\text{Sal}^{\text{OMe}})]^+\text{SbF}_6^-$.

orbitals are strictly orthogonal, so that they cannot overlap. The coupling is then necessary ferromagnetic and the ground spin state of the radical complex $[\text{Cu}(\text{Sal}^{\text{OMe}})]^+$ is paramagnetic ($S = 1$). The zero-field splitting (ZFS) parameters of the triplet are likely larger than 0.3 cm^{-1} because of its X-band silence in the 4–100 K temperature range.^[13] This is confirmed by CASSCF-based ab initio calculations, which predict ZFS parameters of $D = +0.722 \text{ cm}^{-1}$ and $E/D = 0.150$.^[14] In addition, broken-symmetry DFT calculations show that the exchange coupling constant J is large ($+331 \text{ cm}^{-1}$), which evidences a strong ferromagnetic interaction between the metal and the radical, similar to those of $+195$ and $100\text{--}300 \text{ cm}^{-1}$ in bis(*o*-iminobenzosemiquinonato)^[15] and bis(*o*-semiquinonato)^[16] copper(II) complexes, respectively.

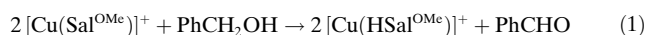
In addition to the copper complexes, the nickel analogues were isolated. The cyclic voltammetry curve of $[\text{Ni}(\text{Sal}^{\text{OMe}})]$ exhibits two anodic responses, at $E_{1/2}^1 = +0.22$ and $E_{1/2}^2 = +0.64$ V versus Fc/Fc^+ , which both correspond to one-electron processes. Electrolysis of $[\text{Ni}(\text{Sal}^{\text{OMe}})]$ results in formation of $[\text{Ni}(\text{Sal}^{\text{OMe}})]^+$, which is EPR-active and exhibits radical bands at 421 and 976 nm.^[10]

Single crystals of $[\text{Ni}(\text{Sal}^{\text{OMe}})]^+\text{SbF}_6^-$ were grown under conditions similar to those used to isolate the copper radical analogue. $[\text{Ni}(\text{Sal}^{\text{OMe}})]^+\text{SbF}_6^-$ exhibits strong structural analogies with $[\text{Cu}(\text{Sal}^{\text{OMe}})]^+\text{SbF}_6^-$ (Figure 1), with a similar quinoid distribution of bond lengths in the ring that has the O2 atom proximal to the SbF_6^- ion. The radical is thus again preferentially localized on one side of the molecule. The spin-density plot calculated by DFT confirms that the SOMO of $[\text{Ni}(\text{Sal}^{\text{OMe}})]^+\text{SbF}_6^-$ is a delocalized π orbital which is mainly

developed on the aromatic ring close to SbF_6^- (63 % contribution). A new important feature, namely, a 10 % contribution from the metal d_{yz} orbital (Figure 2), appears when the radical SOMO of $[\text{Ni}(\text{Sal}^{\text{OMe}})]^+\text{SbF}_6^-$ is compared to that of $[\text{Cu}(\text{Sal}^{\text{OMe}})]^+\text{SbF}_6^-$. Therefore, while the ligand-radical structure is not metal-dependent, the composition of the radical SOMO is.^[17–18]

The 100 K EPR spectrum of electrogenerated $[\text{Ni}(\text{Sal}^{\text{OMe}})]^+$ is characterized by a rhombic ($S = 1/2$) signal with g values of 2.015, 1.992, and 2.054,^[19] which could be nicely reproduced by DFT calculations (computed values $g_{xx} = 2.020$, $g_{yy} = 1.990$, and $g_{zz} = 2.050$). The g_{iso} value of 2.02 is intermediate between those reported for Zn^{II} -coordinated phenoxyl radicals (2.005) and $[\text{Ni}(\text{Sal}^{\text{Bu}})]^+$ (2.04).^[20] This reflects enhanced participation of the ligand in the SOMO, as expected for an increased electron-donating effect of the methoxyl group.

The reactivity of the two radical complexes was studied under single-turnover conditions with the commonly used GO substrate benzyl alcohol. While the stability of electrogenerated $[\text{Cu}(\text{Sal}^{\text{OMe}})]^+$ is noteworthy at 300 K in CH_2Cl_2 ($k_{\text{decomp}} = (0.0044 \pm 0.0001) \text{ min}^{-1}$), it quickly decomposes in the presence of benzyl alcohol. Reduction of the phenoxyl moiety by benzyl alcohol is evident through the disappearance of the radical band in the UV/Vis spectrum and the enhancement in the rate constant resulting from an increase of the alcohol concentration. The plot of the observed rate constant k_{obs} as a function of the benzyl alcohol concentration gave a straight line from which the second-order rate constant $k = (1.2 \pm 0.2) \text{ M}^{-1} \text{ min}^{-1}$ could be extracted. Since no saturation is observed at high benzyl alcohol concentrations, the affinity of the substrate for $[\text{Cu}(\text{Sal}^{\text{OMe}})]^+$ is low, as observed in GO.^[21] Analysis of the reaction products by GC evidenced the formation of (0.5 ± 0.1) equiv of benzaldehyde per complex, while addition of NEt_3 fully restored the spectrum of $[\text{Cu}(\text{Sal}^{\text{OMe}})]$. The reaction thus proceeds as reported by Pratt et al. [Eq. (1)]^[9]



The cation $[\text{Ni}(\text{Sal}^{\text{OMe}})]^+$ is more stable than its copper(II) congener (less than 20 % decomposition after 20 h). In the presence of benzyl alcohol the radical moiety is slowly reduced with a second-order rate constant of $k = (0.040 \pm 0.005) \text{ M}^{-1} \text{ min}^{-1}$. This lack of reactivity is remarkable: It underlines a crucial role of the metal ion in tuning the catalytic properties of $[\text{Ni}(\text{Sal}^{\text{OMe}})]^+$ and $[\text{Cu}(\text{Sal}^{\text{OMe}})]^+$, which exhibit structural analogies and similar oxidizing power.

In conclusion, we have reported the first X-ray crystal structure of a copper(II) radical salen complex and demonstrated that the SOMO is mainly localized on one side of the molecule. Only one structure has been previously reported for a first-row radical salen complex,^[7] but in this nickel complex the SOMO is fully delocalized (class III mixed-valent compound). The structure of $[\text{Ni}(\text{Sal}^{\text{OMe}})]^+$ shows that a localized radical character must alternatively be considered for the nickel compounds in the solid state. Finally, the preference of Nature for copper is not innocent: this metal contributes to maintaining a large amount of spin density on the phenoxyl

group through magnetic coupling. For the nickel complex ($S = 1/2$) a d_{yz} orbital is accessible for accepting part of the spin density. This sharing of the SOMO likely contributes to the lower reactivity of the complex.

Experimental Section

The ligand was obtained by condensation of 3-*tert*-butyl-4-methoxy-2-hydroxybenzaldehyde with (1*R*,2*R*)-(–)-*trans*-1,2-diaminocyclohexane. The neutral complexes were obtained by mixing the ligand with the appropriate metal acetate. $[\text{Cu}(\text{Sal}^{\text{OMe}})]^+\text{SbF}_6^-$ and $[\text{Ni}(\text{Sal}^{\text{OMe}})]^+\text{SbF}_6^-$ were obtained by addition of 1 equiv of AgSbF_6 to a solution of the neutral precursor in CH_2Cl_2 . Elemental analysis calcd (%) for $\text{C}_{30}\text{H}_{40}\text{F}_6\text{N}_2\text{CuO}_4\text{Sb}$ (791.95): C 45.50, H 5.09, N 3.54; found: C 45.90, H 5.15, N 3.71. Elemental analysis calcd (%) for $\text{C}_{30}\text{H}_{40}\text{F}_6\text{N}_2\text{CuO}_4\text{Sb}$: (791.95) C 45.50, H 5.09, N 3.54; found: C 45.90, H 5.15, N 3.71. Elemental analysis calcd (%) for $\text{C}_{30}\text{H}_{40}\text{F}_6\text{N}_2\text{NiO}_4\text{Sb}$ (787.09): C 45.78, H 5.12, N 3.56; found: C 46.03, H 5.23, N 3.62. Experimental, instrumental, crystallographic, and computational details are presented in the Supporting Information.

Received: February 19, 2010

Published online: April 23, 2010

Keywords: copper · enzyme models · nickel · radicals · Schiff base ligands

- [1] J. Stubbe, W. A. Van Der Donk, *Chem. Rev.* **1998**, 98, 705.
- [2] N. Ito, S. E. V. Philips, C. Stevens, Z. B. Ogel, M. J. McPherson, J. N. Keen, K. D. S. Yadav, P. F. Knowles, *Nature* **1991**, 350, 87; M. J. McPherson, M. R. Parsons, R. K. Spooner, C. M. Wilmot, *Handbook of metalloproteins* (Eds.: A. Messerschmidt, R. Huber, K. Wieghardt, T. Poulos), Wiley, Chichester, **2001**; J. W. Whittaker, *Chem. Rev.* **2003**, 103, 2347.
- [3] P. Chaudhuri, K. Wieghardt, *Prog. Inorg. Chem.* **2001**, 50, 151; F. Thomas, *Eur. J. Inorg. Chem.* **2007**, 2379, and references therein.
- [4] In contrast to complexes involving true phenoxyl radicals, crystal structures of complexes with semiquinone or *o*-iminosemiquinone ligands are rather common in the literature due to their higher stability and lower redox potentials.
- [5] A. Sokolowski, E. Bothe, E. Bill, T. Weyhermüller, K. Wieghardt, *Chem. Commun.* **1996**, 1671; Y. Shimazaki, T. D. P. Stack, T. Storr, *Inorg. Chem.* **2009**, 48, 8383.
- [6] L. Benisvy, A. J. Blake, D. Collison, E. S. Davies, C. D. Garner, E. J. L. McInnes, J. McMaster, G. Whittaker, C. Wilson, *Chem. Commun.* **2001**, 1824.
- [7] T. Storr, E. C. Wasinger, R. C. Pratt, T. D. P. Stack, *Angew. Chem.* **2007**, 119, 5290; *Angew. Chem. Int. Ed.* **2007**, 46, 5198.
- [8] Y. Wang, J. L. DuBois, B. Hedman, K. O. Hodgson, T. D. P. Stack, *Science* **1998**, 279, 537; F. Thomas, O. Jarjayes, C. Duboc, C. Philouze, E. Saint-Aman, J.-L. Pierre, *Dalton Trans.* **2004**, 2662; I. Sylvestre, J. Wolowska, C. A. Kilner, E. J. L. McInnes, M. A. Halcrow, *Dalton Trans.* **2005**, 3241; N. Roy, S. Sproules, E. Bothe, T. Weyhermüller, K. Wieghardt, *Eur. J. Inorg. Chem.* **2009**, 2655.
- [9] R. C. Pratt, T. D. P. Stack, *J. Am. Chem. Soc.* **2003**, 125, 8716.
- [10] UV/Vis data for the complexes (λ_{max} [nm] (ϵ [$\text{M}^{-1} \text{ cm}^{-1}$]): $[\text{Cu}(\text{Sal}^{\text{OMe}})]$: 399 (14030), 567 (805); $[\text{Cu}(\text{Sal}^{\text{OMe}})]^+$: 408 (12070), 460 (9930), 555 (2240), > 1100 (> 1600); $[\text{Ni}(\text{Sal}^{\text{OMe}})]$: 334 (8430), 356 sh (7650), 438 (8010), 465 sh (5840); $[\text{Ni}(\text{Sal}^{\text{OMe}})]^+$: 421 (11480), 976 (3430).
- [11] D. Zurita, I. Gautier-Luneau, S. Ménage, J. L. Pierre, E. Saint-Aman, *J. Biol. Inorg. Chem.* **1997**, 2, 46.
- [12] T. Storr, P. Verma, R. C. Pratt, E. C. Wasinger, Y. Shimazaki, T. D. P. Stack, *J. Am. Chem. Soc.* **2008**, 130, 15448.

- [13] A. Dei, D. Gatteschi, L. Pardi, A. L. Barra, L. C. Brunel, *Chem. Phys. Lett.* **1990**, 175, 589.
- [14] These values are within the range of the ZFS determined by high-field EPR for a copper(II) complex of an iminosemiquinone radical.^[12] The dominant contribution to the ZFS is spin-orbit coupling ($D^{\text{SO}} = +0.728 \text{ cm}^{-1}$) with a non-negligible spin-spin part ($D^{\text{SS}} = -0.056 \text{ cm}^{-1}$). The fact that the spin-spin contribution is two orders of magnitude smaller than the total D value shows that the ZFS is mainly due to spin-orbit coupling admixture of excited states into the ground state.
- [15] P. Chaudhuri, C. N. Nazari, E. Bill, E. Bothe, T. Weyhermüller, K. Wieghardt, *J. Am. Chem. Soc.* **2001**, 123, 2213.
- [16] V. I. Ovcharenko, E. V. Gorelik, S. V. Fokin, G. V. Romanenko, V. N. Ikorskii, A. V. Krashilina, V. K. Cherkasov, G. A. Abakumov, *J. Am. Chem. Soc.* **2007**, 129, 10512.
- [17] The shortening of the metal-ligand distances in the nickel complexes results from the smaller ionic radius of the nickel(II) ion compared to the copper(II) ion.
- [18] K. S. Min, T. Weyhermüller, E. Bothe, K. Wieghardt, *Inorg. Chem.* **2004**, 43, 2922.
- [19] Chemically generated $[\text{Ni}(\text{Sal}^{\text{OMe}})]^+\text{SbF}_6^-$ exhibits g values of 2.040, 2.022, and 1.993 ($g_{\text{iso}} = 2.022$). The slight changes in rhombicity show that the counterion interacts with the radical complex.
- [20] Y. Shimazaki, F. Tani, K. Fului, Y. Naruta, O. Yamauchi, *J. Am. Chem. Soc.* **2003**, 125, 10512.
- [21] M. M. Whittaker, J. W. Whittaker, *Biochemistry* **2001**, 40, 7140.